Supersymmetry between deep and shallow optical potentials for $^{16}O+^{16}O$ scattering

J.-M. Sparenberg and D. Baye
Physique Nucléaire Théorique et Physique Mathématique, C.P. 229, Université Libre de Bruxelles, B-1050 Brussels, Belgium
(Received 21 March 1996)

Pairs of supersymmetric transformations allow one to remove square-integrable solutions from a complex potential without modifying its complex phase shifts. This technique is applied to $^{16}O+^{16}O$ scattering where deep and shallow optical potentials provide essentially similar fits of excitation functions over the 10–35 MeV range in the center-of-mass system. After removing complex normalizable solutions from the deep optical potential of Kondō *et al.*, the resulting potential resembles the shallow potential of Chatwin *et al.*, except for the fact that it is singular at the origin. The transformation succeeds in removing bound states and also narrow resonances from the real part of the deep potential. Different theoretical aspects of scattering with complex potentials are also discussed such as the behavior of complex phase shifts in the vicinity of a resonant or normalizable state, and the Levinson theorem. In order to explain phase-shift behaviors, resonance locations are calculated by the complex rotation method, combined with numerical methods valid for determining square-integrable solutions of a Schrödinger equation involving a complex potential. In phase-equivalent pairs of supersymmetric transformations, the apparent contradiction between removing a square-integrable solution which corresponds to a pole of the scattering matrix, and keeping this S matrix unchanged is explained with the Jost function. [S0556-2813(96)00109-4]

PACS number(s): 25.70.Bc, 24.10.Ht, 03.65.Nk

I. INTRODUCTION

The $^{16}O+^{16}O$ system is of particular interest for a study of the interaction between heavy ions. Detailed excitation functions are available at different angles [1,2]. Analyses of these data show that the optical potential is transparent, i.e., that its internal part can be probed with low-energy elastic collisions. A shallow potential, with a common Woods-Saxon form factor for both the real and imaginary parts, could be deduced from data ranging from 10 to 35 MeV in the center-of-mass (c.m.) frame [2]. The quality of the fit has been improved by modifying the treatment of absorption in order to take an explicit account of transparency. Two variants exist: an energy-dependent angular-momentum cutoff [3] or a reduced radius for the Woods-Saxon form factor [4]. The depth of the real part of these potentials is 17 MeV and the fact that the potential is shallow seemed to be established without ambiguity. The shallow nature of the $^{16}O+^{16}O$ interaction was confirmed by a microscopic calculation based on a two-center model with projection on the relative orbital momentum [5]. In that model, the mean value of the microscopic Hamiltonian is assimilated to a nucleus-nucleus potential in a nuclear equivalent of the Born-Oppenheimer approximation. For each partial wave, the microscopic ''potential'' is very close to the common real part of the potentials of Refs. [2–4].

Dynamical microscopic calculations are possible in the framework of variants of the resonating-group method (RGM) [6,7]. When phase shifts for the $^{16}O+^{16}O$ scattering were obtained with this method in a single-channel approximation [8], they displayed an energy dependence which is not compatible with shallow potentials. These phase shifts do not follow the Levinson theorem [9] of a potential without any bound state. The reason for this effect is due to the so-called forbidden states. The nonlocal equations of the RGM allow the existence of a finite number of energy-independent solutions [6,7]. Such solutions correspond to states in the relative motion of the colliding nuclei which are forbidden by the Pauli principle in the full microscopic wave function. An extension of the Levinson theorem due to Swan shows that the number of forbidden states must be added to the number of physical bound states in the calculation of the difference between the phase shifts at zero and infinite energies [10]. Detailed analyses of the microscopic model indicate that a potential reproducing RGM phase shifts must be deep [11]. It is therefore not surprising that attempts to derive a deep $^{16}O+^{16}O$ potential agreeing with the microscopic interpretation became successful [12,13]. These potentials have a squared Woods-Saxon form factor for the real part and an imaginary part of the same type as in the shallow potential of Ref. [3]. Such a potential now exists not only in the energy range where the shallow potential is available but also at $E_{\mathrm{c.m.}}=175$ MeV [14] and $E_{\mathrm{c.m.}}=72.5$ MeV [15]. Although the shape slightly varies with energy, the different deep potentials obviously belong to a unique family [15].

In fact, the same evolution had already been encountered in the analysis of the much simpler $\alpha+\alpha$ scattering. Early potentials were shallow and angular-momentum dependent [16,17]. They did however not follow the same Levinson theorem as microscopically derived phase shifts [6,7]. An energy-independent deep potential based on the correct number of forbidden states was proposed in 1971 [18]. These efforts became totally successful with the derivation of a two-parameter deep Gaussian potential able to reproduce all the $\alpha+\alpha$ phase shifts up to $E_{\mathrm{c.m.}}=20$ MeV [19]. The coexistence of deep l-independent and shallow l-dependent potentials can be explained using supersymmetric transformations [20]. Supersymmetry allows one to ''remove'' all bound states from a real potential without affecting the phase shifts. The deep potential of Ref. [19] is transformed into a phase-equivalent shallow potential very close to the potential of Ref. [17]. However, the transformed potential presents an

r^{-2} singularity at the origin which allows it to follow the same Levinson theorem as the deep potential. Indeed, another theorem due to Swan shows how this singularity affects the phase-shift variation [21]. The shallow potential of Ref. [17] can be considered as a regular approximation of the singular potential equivalent to the deep potential of Ref. [19].

The technique of supersymmetric transformations has received several generalizations in the context of real potentials [22–25]. The complex case was more delicate because it did not seem possible to remove bound states from the real part without modifying the phase shifts. Recently, however, it was realized that the same goal can be reached by removing *complex* ''bound states,'' i.e., normalizable solutions of the Schrödinger equation with the full complex potential [26]. Let us stress here that these complex normalizable solutions do not have a direct physical meaning in the case of an optical potential. They do not imply the existence of any physical bound system. Bound states of the *real* part of this potential, at negative energies, can sometimes be interpreted as approximate physical states of the fused nucleus. Narrow resonances of this real part are in principle observable. However the square-integrable solutions of the complex optical potential are meaningless since the imaginary part is only used to simulate the flux removal from the elastic channel due to other open channels. The real parts of the corresponding energies may resemble the physical energies of bound states or resonances and their imaginary parts may be related to widths of structures observed in the phase shifts. Anyway, the application of this new technique to different solvable potentials and to the $\alpha+{}^{16}\mathrm{O}$ elastic scattering [26] has shown that removing complex normalizable states transforms a deep potential into a shallow one, without affecting the scattering properties of this potential. The aim of the present paper is to apply this technique to the well-documented ${}^{16}\mathrm{O}+{}^{16}\mathrm{O}$ case and to make a comparison between the two families of optical potentials. We shall compare the potential of Kondo, Robson, and Smith [12] with a shallow potential valid over the same energy range, with the same type of absorption, i.e., the potential of Chatwin, Eck, Robson, and Richter [3]. Since the supersymmetry method can be applied to l-dependent potentials but not to energy-dependent ones, we shall perform the comparison at different fixed energies.

The principle of supersymmetric transformations and the necessary algorithms are summarized in Sec. II. The problem is specialized to the ${}^{16}\mathrm{O}+{}^{16}\mathrm{O}$ case. Section III can be skipped by the reader interested in ${}^{16}\mathrm{O}+{}^{16}\mathrm{O}$ results only. It contains a more detailed analysis of collision-matrix properties for complex potentials. In particular, the influence of complex square-integrable states and of resonances on phase shifts is discussed, the relevant Levinson theorem is presented and the origin of phase equivalence in supersymmetric transformations is elucidated on the Jost function. The physical comparison between the ${}^{16}\mathrm{O}+{}^{16}\mathrm{O}$ potentials is performed in Sec. IV. The origin of the phase-shift behavior is clarified. Concluding remarks are presented in Sec. V.

II. PRESENTATION OF THE METHOD

A. Basic definitions

Let us first recall some definitions related to elastic scattering with a complex optical potential. For $\hbar^2/2\mu=1$ (where μ is the reduced mass of the system), the radial Schrödinger equation at orbital momentum l, for any complex energy $E=k^2$, reads

$$\left(-\frac{d^2}{dr^2}+V^l(r)\right)\psi^l(k,r)=k^2\psi^l(k,r). \tag{1}$$

The complex effective potential $V^l(r)=U^l(r)+iW^l(r)$, where W^l is negative, behaves asymptotically as

$$V^l(r)\underset{r\to\infty}{\to}\frac{l(l+1)}{r^2}+\frac{2\eta k}{r}, \tag{2}$$

where $\eta=Z_1Z_2e^2/2k$ is the Sommerfeld parameter. This potential is bounded except possibly near the origin. Near $r=0$, it behaves as

$$V^l(r)\underset{r\to 0}{\to}\frac{\nu^l(\nu^l+1)}{r^2}, \tag{3}$$

where ν^l is a positive integer. For regular potentials, such as those in Refs. [3,12], ν^l is equal to l. In the following, we shall also use singular potentials with $\nu^l\neq l$ resulting from supersymmetric transformations. The superscript l appearing in the different notations refers to the orbital momentum of the partial wave, which is not affected by the supersymmetric transformations considered in the following.

Let $\psi^l(k,r)$ be a solution of Eq. (1) vanishing at the origin. If, for some complex energy $E_0=k_0^2$, this solution also vanishes at infinity, the potential is said to have a normalizable solution at E_0.

For positive energies ($k>0$), a physical wave function is a solution of Eq. (1) regular at $r=0$ with the asymptotic behavior

$$\psi^l(k,r)\underset{r\to\infty}{\to}\sin(kr-\tfrac{1}{2}l\pi-\eta\ln 2kr+\sigma^l(k)+\delta^l(k)), \tag{4}$$

where $\sigma^l(k)=\arg\Gamma(l+1+i\eta)$ is the Coulomb phase shift, and $\delta^l(k)$ is the complex additional or quasinuclear phase shift, defined by Eq. (4) up to a multiple of π.

From the Coulomb and additional phase shifts, one deduces the S matrix

$$\begin{aligned}S^l(k)&=\exp[2i\sigma^l(k)]\exp[2i\delta^l(k)]\\&=\exp[2i\sigma^l(k)]A^l(k)\exp[2i\xi^l(k)].\end{aligned} \tag{5}$$

For real k, the reflection coefficient $A^l(k)$ and phase $\xi^l(k)$ are real. For a real potential, the additional phase shift $\delta^l(k)$ is real and the reflection coefficient is unity. The phase shifts allow one to calculate the elastic scattering cross sections [9].

B. Optical potentials for ${}^{16}\mathrm{O}+{}^{16}\mathrm{O}$ scattering

Let us now present the two potentials $V^l(r)$ which provide a good fit of the elastic ${}^{16}\mathrm{O}+{}^{16}\mathrm{O}$ excitation functions, in the energy range 10 MeV$<E_{\mathrm{c.m.}}<$35 MeV. In addition to the centrifugal term and to a point-sphere Coulomb potential, they both contain energy-dependent and angular-momentum-dependent imaginary parts with a Woods-Saxon form factor.

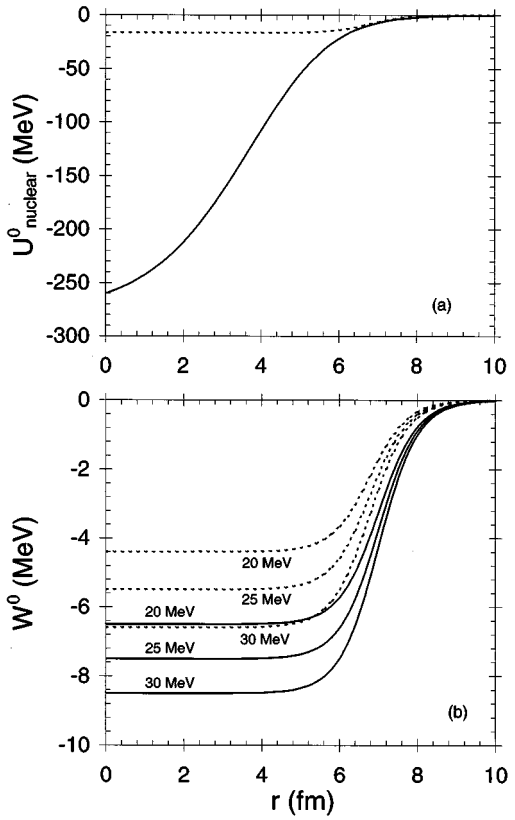

FIG. 1. Potentials of Chatwin *et al.* (Ref. [3], dotted lines) and of Kondō *et al.* (Ref. [12], full lines) for $l=0$ at 20, 25, and 30 MeV.

However, the shapes and depths of their real parts are significantly different as discussed in the Introduction.

The potential of Chatwin *et al.* [3] improves an earlier potential of Maher *et al.* [2] with the introduction of a more elaborate imaginary part depending on both energy and angular momentum. For $l=0$, it is represented by dotted lines in Fig. 1, at 20, 25, and 30 MeV. Its real part neither depends on energy nor on angular momentum. The depth of the imaginary part increases with energy, in agreement with the increasing number of nonelastic channels. With a depth of about 17 MeV, the *real* part of this ''shallow'' potential does not support any bound state. However we shall see later that the whole *complex* potential has normalizable solutions, connected to resonances of its real part, because of the increase of its imaginary part with energy. These solutions have no precise physical meaning but play a definite role in the energy dependence of the phase shifts.

The second potential, introduced by Kondō *et al.* in 1989 [12], has an imaginary part very similar to that of the preceding potential. Its real part has a squared Woods-Saxon shape with a depth of about 260 MeV and slightly depends on angular momentum. The $l=0$ nuclear potential is also represented in Fig. 1 (full lines), for the same energies. The real part of this ''deep'' potential has several bound states. We shall see later that these bound states correspond to normalizable solutions of the whole complex potential, but that some other normalizable solutions, related to resonances of the real part, also occur.

C. Supersymmetry between deep and shallow optical potentials

Very different phenomenological potentials can reproduce the same experimental data. Actually, both potentials not only share approximately the same cross sections, but also nearly share the same phase shifts (see Sec. IV). How can so different potentials, with so different bound spectra, share the same phase shifts? This question is answered by supersymmetry: removing a normalizable solution from a deep potential with a pair of supersymmetric transformations provides a shallower potential without modifying phase shifts. In some cases, the shallow potential obtained after several iterations is very similar to a shallow phenomenological potential [20]. With a method generalized to complex potentials [26], this will also happen for the $^{16}O+^{16}O$ scattering.

A supersymmetric or Darboux transformation is based on a factorization of the Hamiltonian into two first-order differential operators [27]. It makes use of a solution of the Schrödinger equation (the factorization solution) at a certain energy (the factorization energy) and generates a new potential which shares the bound spectrum of the initial potential, except possibly at the factorization energy. In the case of interest for the present work, two successive transformations are performed, with the same factorization energy. The first transformation uses a square-integrable solution of the initial potential $V_0^l(r)$. The resulting potential $V_1^l(r)$ has one normalizable state less (at the factorization energy), but does not have the same phase shifts as $V_0^l(r)$. A second transformation restores the initial phase shifts. This second transformation uses a nonphysical solution of $V_1^l(r)$, vanishing at the origin, but exponentially increasing at infinity.

Let $\psi_0^l(k_0,r)$ be a normalizable solution of $V_0^l(r)$ at the complex energy $E_0=k_0^2$. The potential resulting from the pair of supersymmetric transformations reads [22,26]

$$V_2^l(r)=V_0^l(r)-2\frac{d}{dr}\left(\frac{\psi_0^l(k_0,r)^2}{\int_0^r\psi_0^l(k_0,t)^2dt}\right). \tag{6}$$

The solutions of the new Schrödinger equation at any energy can also be expressed in terms of solutions of the initial equation as

$$\psi_2^l(k,r)=\psi_0^l(k,r)-\psi_0^l(k_0,r)\frac{\int_0^r\psi_0^l(k_0,t)\psi_0^l(k,t)dt}{\int_0^r\psi_0^l(k_0,t)^2dt}. \tag{7}$$

In particular, for real positive energies, this implies up to a multiple of π

$$\delta_2^l(k)=\delta_0^l(k) \tag{8}$$

since the second term in the right-hand side of Eq. (7) vanishes at infinity. Potentials $V_0^l(r)$ and $V_2^l(r)$ satisfying Eq. (8) are said to be phase equivalent. Equation (7) also shows that $\psi_2^l(k_0,r)$ vanishes. Normalizable solutions do not exist any more at energy E_0. This energy is ''removed'' from the spectrum of the complex potential V_2^l. This removal usually corresponds to a reduction of the real-part depth. The new potential is shallower than the original one.

Relation (6) can be iterated in order to remove several square-integrable solutions from a potential. Starting from a solution $\psi_2^l(k_1,r)$ of V_2^l at an energy $E_1=k_1^2$ where the initial potential V_0^l has another normalizable solution, one can transform V_2^l into V_4^l, and so on. The potential V_{2n}^l is obtained when n normalizable solutions are removed. Starting from a deep potential with a number of bound states (or narrow resonances as we shall see in Sec. IV) supported by its real part, one can obtain an equivalent shallow potential.

As in the real case [23], compact formulas based on determinants involving normalizable solutions of the initial potential can be derived in place of these iterations. Moreover, the problem considered here, i.e., removing normalizable solutions, can be extended to adding such solutions, modifying their energy, and any combination of such modifications, by generalizing the contents of Refs. [22–25].

In the present application, we limit ourselves to the removal of normalizable states. When several such states have to be removed, we iterate formula (6) rather than use a compact formula for the final potential: this allows us to check the intermediate potentials and their phase shifts.

The numerical implementation of formula (6) is rather simple: we first have to find the complex eigenvalues and the corresponding normalizable solutions of potential V_0^l. In Ref. [26], two numerical methods are found to be efficient in determining these solutions. The first one is based on finite differences, while the second one uses Lagrange meshes [28,29]. The implementation of formula (6) then only requires traditional integration and differentiation numerical methods.

III. *S*-MATRIX PROPERTIES

The reader mostly interested by the physical application of supersymmetry to $^{16}O+^{16}O$ scattering may directly proceed to Sec. IV. The subjects covered here are more mathematical and not essential for applying our method. They are however useful to understand in detail the behavior of the phase shifts of a complex potential, and the way they are kept unchanged by supersymmetric transformations.

A. Jost function and *S* matrix

For any complex k, the Jost solutions of Eq. (1) are uniquely defined by their asymptotic behavior

$$f^l(\pm k,r) \underset{r\to\infty}{\to} \exp[i\tfrac{1}{2}\nu^l\pi \pm ikr \mp i\eta\ln(\mp 2ikr)], \tag{9}$$

with a cut along the negative imaginary k axis. In this expression k, ik, and $-ik$ are related by

$$-ik=\exp(-i\tfrac{1}{2}\pi)k=\exp(-i\epsilon\pi)ik, \tag{10}$$

where $\epsilon=\mathrm{sgn}\ \mathrm{Re}k$. These conventions keep the argument of the complex number in the logarithm between $-\pi$ and π. Except for the phase factor $\exp[i(1/2)\nu^l\pi]$ which is introduced for convenience, Eq. (9) is inspired as in Ref. [30] by the asymptotic form of the Jost solutions for the pure Coulomb case

$$f_C^l(\pm k,r)=\exp(i\tfrac{1}{2}l\pi)W_{\mp i\eta,l+\frac{1}{2}}(\mp 2ikr), \tag{11}$$

where $W_{\kappa,\mu}$ is a Whittaker function [31]. In Ref. [9], the Jost solutions for the Coulomb case are defined with a different normalization and only for $\mathrm{Re}k>0$.

Near the origin, the functions $f^l(\pm k,r)$ are in general proportional to $r^{-\nu^l}$. They are linearly independent since

$$W(f^l(k,r),f^l(-k,r))=(-1)^{\nu^l+1}2ik\exp(-\epsilon\eta\pi), \tag{12}$$

where $W(f,g)$ is the Wronskian $fg'-f'g$.

The regular solution $\varphi^l(k,r)$ is the solution of Eq. (1) satisfying

$$\varphi^l(k,r) \underset{r\to 0}{\to} \frac{r^{\nu^l+1}}{(2\nu^l+1)!!}. \tag{13}$$

It is even in k as a solution of the even equation (1) and boundary condition (13). Let us write it as a linear combination of the Jost solutions

$$\varphi^l(k,r)=\tfrac{1}{2}ik^{-\nu^l-1}\exp(\epsilon\eta\pi)[F^l(k)f^l(-k,r) -(-1)^{\nu^l}F^l(-k)f^l(k,r)]. \tag{14}$$

It defines the Jost function $F^l(k)$, which is dimensionless. Using Eqs. (12)–(14), the Jost function can also be written as

$$F^l(k)=(-k)^{\nu^l}W(f^l(k,r),\varphi^l(k,r)) =\frac{(-k)^{\nu^l}}{(2\nu^l-1)!!}\lim_{r\to 0} r^{\nu^l}f^l(k,r). \tag{15}$$

In the pure Coulomb case, Eqs. (15) and (11) provide the Jost function

$$F_C^l(k)=\Gamma(l+1)/\Gamma(l+1+i\eta), \tag{16}$$

which tends towards 1 when $|k|$ tends to infinity.

In the general case of a complex potential, the Jost function has no particular symmetry, whereas it verifies the relation

$$F^l(-k^*)=F^l(k)^* \quad (V^l \text{ real}) \tag{17}$$

for a real potential [9,32]. The S matrix is defined for any complex k by

$$S^l(k)=F^l(-k)/F^l(k). \tag{18}$$

It has the symmetry property

$$S^l(-k)=S^l(k)^{-1} \tag{19}$$

and, for a real potential, one deduces from Eq. (17),

$$S^l(-k^*)=S^l(k)^* \quad (V^l \text{ real}). \tag{20}$$

In particular, the S matrix for the Coulomb case reads

$$S_C^l(k)=\exp(2i\sigma^l(k))=\Gamma(l+1+i\eta)/\Gamma(l+1-i\eta). \tag{21}$$

The Coulomb phase shift $\sigma^l(k)$ is an odd function of k.

In the general case of a Coulomb plus short-range potential, let us factorize the Jost function as

$$F^l(k)=F^l_C(k)G^l(k)\exp[-i\delta^l(k)], \tag{22}$$

where $F^l_C(k)$ is given by Eq. (16) and where $G^l(k)$ and $\delta^l(k)$ are, respectively, even and odd functions of k. With Eq. (18) and this definition, the first expression (5) of the scattering matrix is recovered for complex k. The function $\delta^l(k)$ introduced in Eq. (22) extends the complex phase shift to complex k values. When $|\nu^l-l|$ is even as in pairs of supersymmetric transformations (see Sec. III E), it is equivalent to the phase shift defined in Eq. (4). With Eq. (9), Eqs. (14) and (22) provide the asymptotic behavior (4) for k real, up to a multiplicative factor.

B. Normalizable states and Levinson theorem

Equations (14) and (9) show that Eq. (1) has a square-integrable solution at energy $E_0=k_0^2$, if and only if $F^l(k_0)=0$ for $\mathrm{Im}k_0>0$. For real potentials, the energies of normalizable solutions have to be real and negative, whereas for complex potentials, they are complex and their real part is either negative or positive (see Ref. [26] and references therein).

Equation (18) shows that a zero of F^l in $\{\mathrm{Im}k>0\}$ implies a pole of S^l in $\{\mathrm{Im}k>0\}$, whereas a pole of S^l does not necessarily imply a zero of F^l: it can correspond to a pole of F^l in $\{\mathrm{Im}k<0\}$. In other words, the S matrix may have a pole in $\{\mathrm{Im}k>0\}$ which does not correspond to any normalizable solution. For instance, this is the case with some potentials derived from supersymmetric transformations (see Sec. III E).

The Levinson theorem [9,32] establishes a link between the number n^l of bound states and the phase shift $\delta^l(k)$ of a real regular potential decreasing faster than r^{-2} for r tending towards infinity. It was extended to the Coulomb case [33] and generalized [21] to potentials with a singularity at the origin. In the former case, the theorem applies to the additional phase shift, i.e., to the difference between the total and Coulomb phase shifts. Proofs for short-range regular potentials in the real case can be transposed without significant modification to complex potentials. Taking into account all these generalizations, we conjecture a theorem valid for all complex potentials containing a Coulomb term and a possible r^{-2} singularity at the origin. It reads

$$A^l(0)=A^l(\infty)=1,$$

$$\xi^l(0)=[n^l+\tfrac{1}{2}(\nu^l-l)]\pi,$$

$$\xi^l(\infty)=0, \tag{23}$$

where n^l is the number of normalizable solutions. Here we do not follow Swan's convention [21], where $\xi^l(0)=n^l\pi$. With the present convention, the phase shift remains unchanged after pairs of supersymmetric transformations (see Sec. III E). The theorem may have to be modified in the s wave when a square-integrable state exists at zero energy [32], but this case does not occur when the potential contains a Coulomb term [33].

Let us finally emphasize that this theorem only applies to potentials which do not depend on energy. Therefore, it is not valid for the $^{16}O+^{16}O$ potentials discussed in Sec. II B but it can be helpful when these potentials are considered at a fixed energy, as studied in Sec. IV A.

C. Influence of normalizable states and resonances on the complex phase shift

Zeros of the Jost function in $\{\mathrm{Im}k>0\}$ correspond to square-integrable solutions. The Jost function $F^l(k)$ can also have zeros in $\{\mathrm{Im}k<0\}$, leading to poles of the S matrix. These zeros are not associated with square-integrable solutions of Eq. (1); they correspond to resonances. If they are close enough to the real axis, their presence can have an influence on the phase shift.

A very important difference between complex and real potentials is the fact that, for complex potentials, square-integrable states can also have an influence on the phase shift at positive energies. The zeros of the Jost function in $\{\mathrm{Im}k>0\}$ must be close enough to the real axis. For real potentials, the reality of bound-state energies leads to zeros of F^l on the positive imaginary k axis. Therefore they can only have an influence on the phase shift near $E=0$.

Consequently, a systematic study of the phase-shift behavior near a pole of the S matrix is also necessary for a complex potential. The simplest way to establish it is to expand S near its poles and zeros [32]. For a *resonance* of a *real* potential at k_0, with $\mathrm{Im}k_0<0$, the S matrix has poles at k_0 and $-k_0^*$, and zeros at k_0^* and $-k_0$. On the real k axis, in the neighborhood of $\pm\mathrm{Re}k_0$, the S matrix can be written as

$$S^l(k)=\exp[2i\delta^l_{bg}(k)]\frac{k+k_0}{k-k_0}\frac{k-k_0^*}{k+k_0^*}\quad (V^l \text{ real}), \tag{24}$$

in agreement with the symmetry relations (19) and (20). In this expression, δ^l_{bg} is a background phase shift, which is real since the potential is real. The resonant part of the phase shift is given by half the phase of the second and third factors; it increases by π as k increases past $|\mathrm{Re}\,k_0|$.

For a *resonance* of a *complex* potential at k_0, with $\mathrm{Im}k_0<0$, the S matrix has only a pole at k_0 and a zero at $-k_0$, in agreement with Eq. (19); relation (20) is not verified any more. The S matrix along the real k axis is thus in this case

$$S^l(k)=\exp[2i\delta^l_{bg}(k)]\frac{k+k_0}{k-k_0}. \tag{25}$$

The second factor corresponds to a *complex* resonant phase shift. Let us study its behavior on the positive real axis, near $|\mathrm{Re}k_0|$. Equation (25) shows that $A^l(k)$ has a maximum near $|\mathrm{Re}k_0|$ when $\mathrm{Re}k_0>0$ or a minimum when $\mathrm{Re}k_0<0$. As k increases beyond $|\mathrm{Re}k_0|$, $\xi^l(k)$ increases of $\pi/2$ (not π). These behaviors are schematically represented in Fig. 2 for $\delta^l_{bg}=0$.

The behavior of a resonance of a *real* potential can be interpreted as the combined effect of two poles of the S matrix, one with $\mathrm{Re}k_0<0$ and one with $\mathrm{Re}k_0>0$. Each of them leads to an increase of $\pi/2$ in the real part ξ^l of the

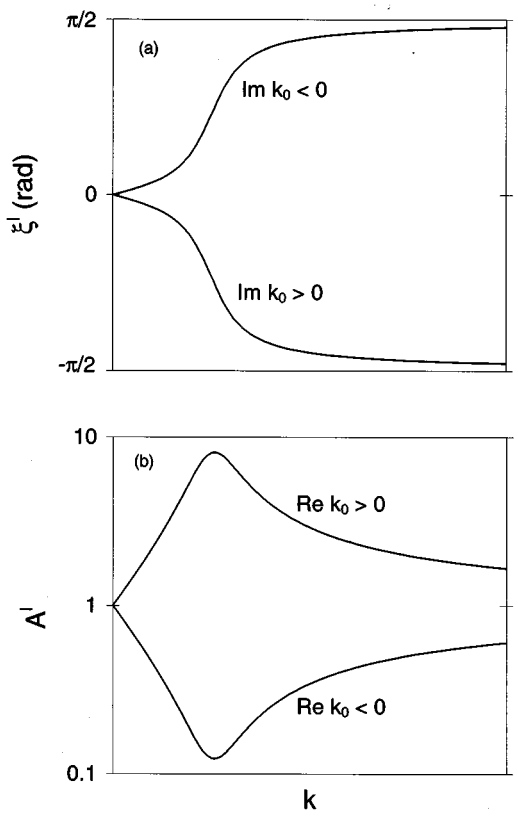

FIG. 2. Schematic behavior of the phase ξ^l and modulus A^l of the quasinuclear scattering matrix near a normalizable-state ($\mathrm{Im}k_0>0$) or resonance ($\mathrm{Im}k_0<0$) pole located at k_0.

phase shift, but with compensating effects on its imaginary part and hence on the reflection coefficient A^l which remains equal to unity.

For a *normalizable state* of a *complex* potential at k_0, with $\mathrm{Im}k_0>0$, the S matrix has a pole at k_0 and a zero at $-k_0$ as in the preceding case. Expansion (25) of S shows that $A^l(k)$ has the same behavior as for a resonance, but that the real part $\xi^l(k)$ of the resonant phase shift behaves differently: it *decreases* by $\pi/2$ as k increases past $|\mathrm{Re}k_0|$. The possible behaviors are also schematically represented in Fig. 2.

A pair of poles at k_0 and in the close vicinity of $-k_0$ introduces two inverse factors whose product is close to unity. In this case, the effect of these poles is weak and the phase shift reduces to its background value. It should be noted that the effect of a pole with $\mathrm{Re}k_0>0$ is always compensated by other poles in such a way that $A^l(k)$ remains smaller than unity as required by the negative imaginary part of the potential. This type of behavior is for example observed on phase shifts obtained with a phenomenological potential fitting $^{12}\mathrm{C}+^{16}\mathrm{O}$ cross sections (see Fig. 2 in Ref. [34]). Complex potentials are able to simulate the well-known variations of a scattering matrix in the vicinity of a resonance in the presence of two open channels [6,35]. Such behaviors are also reported for optical potentials used for Σ hypernuclear states in Ref. [36].

For a complex potential, a third case can in principle occur: the S matrix may have a pole *on* the real axis. This is just the intermediate case between the previous cases, and the behavior of the phase shift can be deduced from the preceding discussions: $\xi^l(k)$ has a discontinuity of $\pi/2$ at $|k_0|$, and $A^l(k)$ has a pole or a zero depending on whether $\mathrm{Re}\,k_0$ is positive or negative.

D. Numerical calculation of resonance energies

The numerical methods of Ref. [26] mentioned above only allow one to calculate normalizable-state energies, i.e., poles of the S matrix in the upper half k plane. However, since these energies are already complex, these methods can be directly generalized to calculate resonance energies, by using the complex rotation technique [37]. Replacing r by $e^{i\theta}r$ in Eq. (1) and multiplying by $e^{2i\theta}$ lead to a new Schrödinger equation

$$\left(-\frac{d^2}{dr^2}+e^{2i\theta}V^l(e^{i\theta}r)\right)\psi^l(k,e^{i\theta}r)=e^{2i\theta}k^2\psi^l(k,e^{i\theta}r). \tag{26}$$

In the following, $V^l(e^{i\theta}r)$ is assumed to be bounded for $r>0$.

Let $\psi^l(k_0,r)$ be a solution of Eq. (1), vanishing at the origin but not normalizable, corresponding to a zero of the Jost function (and hence to a pole of the S matrix) at k_0 with $\mathrm{Im}\,k_0\leqslant 0$. Then $\psi^l(k_0,e^{i\theta}r)$ is a solution of Eq. (26). Using expression (14) and the asymptotic behavior (9), one has

$$\psi^l(k_0,e^{i\theta}r)\propto f^l(k_0,e^{i\theta}r)$$

$$\underset{r\to\infty}{\to}\exp[i\mathrm{Re}(k_0e^{i\theta})r]\exp[-\mathrm{Im}(k_0e^{i\theta})r], \tag{27}$$

where for simplicity we neglect constant and logarithmic terms with respect to linear terms in the arguments of exponentials. Equation (27) shows that the solution $\psi^l(k_0,e^{i\theta}r)$ is normalizable when θ satisfies the condition

$$\mathrm{Im}(k_0e^{i\theta})>0. \tag{28}$$

The complex rotation technique has changed a resonance into a square-integrable state, and the energy of this state can be calculated by solving Eq. (26) with the techniques of Ref. [26].

For any k_0, condition (28) can be fulfilled for $-(1/2)\pi<\theta<(1/2)\pi$. In traditional presentations of the complex rotation method for real potentials, one searches the resonances in $\{\mathrm{Re}k>0\}$ and one makes use of positive values of θ. Since a real potential has symmetric resonances with respect to the imaginary k axis, the complex rotation method could also be used to find the resonances in $\{\mathrm{Re}k<0\}$ with negative θ values. In the following, we need both positive and negative θ values since the resonances of a complex potential are not symmetric any more.

E. Modification of the Jost function by supersymmetry

Let us first establish formula (7) in more detail. For a single supersymmetric transformation with a factorization function $\psi_0^l(k_0,r)$ regular at the origin, the solutions of the

transformed potential can be expressed in terms of the solutions of the initial potential in two different manners [22]

$$\psi_1^l(k,r) = -(k^2-k_0^2)^{-1/2}\frac{W(\psi_0^l(k_0,r),\psi_0^l(k,r))}{\psi_0^l(k_0,r)} \quad (29)$$

or

$$\psi_1^l(k,r) = (k^2-k_0^2)^{1/2}\frac{\int_0^r \psi_0^l(k_0,t)\psi_0^l(k,t)dt}{\psi_0^l(k_0,r)}. \quad (30)$$

Formula (7) is obtained by choosing the integral formulation (30) for the first transformation (which removes the normalizable state), and (up to a phase factor) the Wronskian or differential formulation (29) for the second transformation (which restores the initial phase shift). In the second step, $\psi_0^l(k_0,r)$ is replaced by the solution $[\psi_0^l(k_0,r)]^{-1}\int_0^r \psi_0^l(k_0,t)^2 dt$, vanishing at the origin but increasing at infinity, of the transformed Schrödinger equation at energy E_0.

Using Eq. (30) twice allows us to compare the behaviors of solutions near the origin. Since $\psi_0^l(k,r)$ behaves like $r^{\nu_0^l+1}$, leading terms of series expansions show that $\psi_2^l(k,r)$ behaves like $r^{\nu_0^l+3}$. Therefore the singularity parameter ν_2^l of potential V_2^l increases by two units,

$$\nu_2^l = \nu_0^l + 2. \quad (31)$$

The strength $\nu^l(\nu^l+1)$ of the potential singularity at the origin increases at each state removal. This explains how successive potentials can provide the same phase shifts with different numbers of normalizable states. They all verify the generalized Levinson theorem (23). They share the same $\xi^l(0)$ in spite of different n^l and ν^l values, because of a common sum $n^l+(1/2)\nu^l$.

Equations (29) and (30) remain valid when $\psi_0^l(k,r)$ is replaced by a nonphysical solution behaving like $r^{-\nu^l}$ near the origin [23]. Consequently, Eq. (7) is also valid for this kind of solution. As seen in Sec. II C, Eq. (7) clearly reveals the phase equivalence since the physical solutions $\psi_0^l(k,r)$ and $\psi_2^l(k,r)$ (k real) have exactly the same asymptotic behavior. The same argument applies to the nonphysical Jost solutions $f_0^l(k,r)$ and $f_2^l(k,r)$. According to Eq. (31), these solutions follow exactly the same asymptotic behavior and normalization (9) up to a sign. The transformed Jost solution $f_2^l(k,r)$ is thus expressed in terms of $-f_0^l(k,r)$ with Eq. (7). Equivalently, applying Eqs. (29) and (30) to $f_0^l(k,r)$ provides $f_2^l(k,r)$.

Near the origin, the Jost solution $f_0^l(k,r)$ behaves as $Cr^{-\nu_0^l}$, where C is related to the Jost function $F_0^l(k)$ through Eq. (15). Using Eq. (29) twice provides the transformed Jost function $F_2^l(k)$. The solution in the intermediate step, which is not normalized as in Eq. (9), behaves near the origin as $(k^2-k_0^2)^{-1/2}(2\nu_0^l+1)Cr^{-\nu_0^l-1}$. The final solution, which is the Jost solution $f_2^l(k,r)$, behaves as $(k^2-k_0^2)^{-1}(2\nu_0^l+1)(2\nu_0^l+3)Cr^{-\nu_0^l-2}$. From Eqs. (15) and (31), the Jost function $F_2^l(k)$ of the transformed potential $V_2^l(r)$ is then deduced as

$$F_2^l(k) = \frac{k^2}{k^2-k_0^2}F_0^l(k). \quad (32)$$

This equation shows that (i) the zero of the Jost function at k_0 is removed, (ii) a pole of the Jost function appears at $-k_0$, and (iii) the S matrix defined in Eq. (18) remains unchanged after the transformation pair,

$$S_2^l(k) = S_0^l(k), \quad (33)$$

which confirms Eq. (8). For the singular transformed potential V_2^l, the zeros of the Jost function and the poles of the S matrix are not identical. Removing a normalizable solution without modifying the S matrix implies replacing a zero of the Jost function by a pole.

IV. APPLICATION TO ^{16}O+^{16}O SCATTERING

A. Properties of the potential of Kondō *et al.*

The potential of Ref. [12], which fits elastic scattering data for ^{16}O+^{16}O in the energy range 10 MeV $< E_{\text{c.m.}} <$ 35 MeV, depends on angular momentum and energy. Supersymmetric transformations can be performed for each partial wave separately but assume that the potential does not depend on energy. To this end, we first freeze the energy dependence of the potential at 25 MeV and focus on the dominant $l=18$ partial wave at this energy [4]. The $l=18$ effective potential for $E_{\text{c.m.}}=25$ MeV is represented in Fig. 5 (thick line).

In order to apply supersymmetric transformations, we need the complex energies of the square-integrable states of this potential. For completeness, we also consider its resonances and phase-shift properties. Figure 3 shows the first poles of the $l=18$ S matrix (zeros of the Jost function) in the complex k and E planes (full dots). The poles are numbered by increasing real parts of the energy; a letter indicates whether the pole corresponds to a normalizable state (N,Im$k_0>0$) or to a resonance (R,Im$k_0<0$). Empty dots represent the poles related to the real part of the effective potential.

Poles above the real k axis, which correspond to square-integrable solutions of Eq. (1), are calculated with the finite-difference technique presented in Ref. [26]. An accuracy of about 10^{-6} is achieved with 2000 points and a step of 0.01 fm. Poles under the real k axis, which correspond to resonances, are calculated with the same technique, combined with the complex rotation method, as explained in Sec. III D. This method requires an analytic continuation of the potential of Kondō *et al.* in the complex plane. This continuation is obvious for the nuclear and centrifugal terms, which both have infinitely differentiable analytic expressions, but does not rigorously exist for a point-sphere Coulomb potential. We obtain satisfactory results with a piece-analytic potential, discontinuous at $|z|=R_C$, where R_C is the radius of the charged sphere. As an example, resonance $R6$ requires a minimum rotation angle of $-4.78°$. This angle has to be negative as discussed in Sec. III D (see also Fig. 3). An ac-

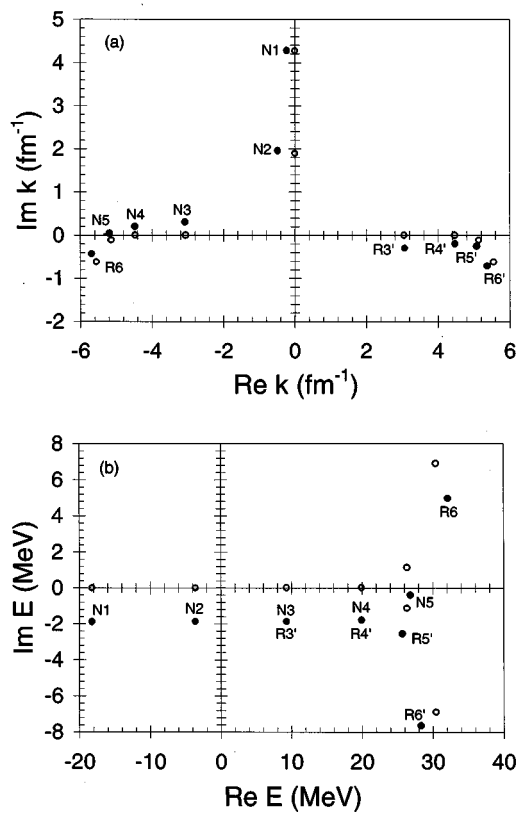

FIG. 3. Poles of the $l=18$ S matrix for the deep potential of Ref. [12] at 25 MeV in the complex k and E planes (full dots). The poles of normalizable states (N) or resonances (R) are numbered by increasing real parts of their energy. Empty dots represent the poles of the real part U^{18} of the effective potential.

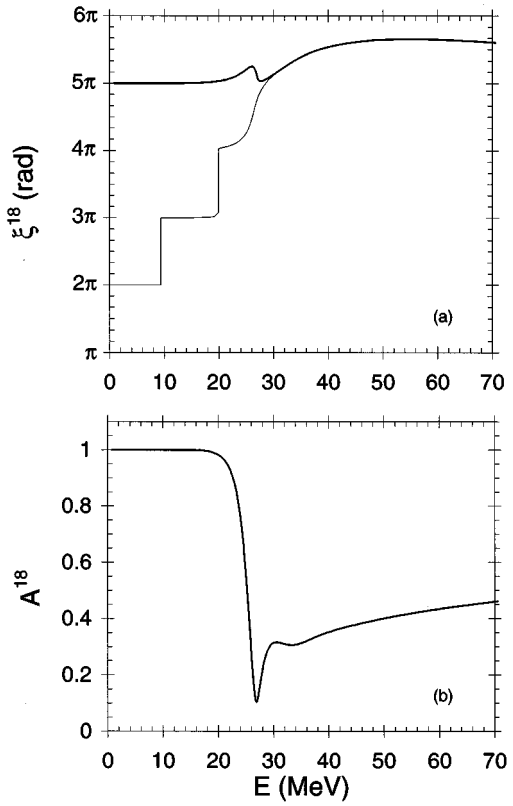

FIG. 4. $l=18$ phase shift of the real part of the potential of Ref. [12] at 25 MeV (thin line), and phase and modulus of the S matrix for the full complex potential (thick lines).

curacy of 10^{-3} can be obtained for slightly larger angles ($>-4.9°$). The locations of poles $R5$' and $R6$' are not easily determined. For these poles, the angle has to be positive. Starting from the corresponding poles of the real part of the potential is helpful.

The real part of the potential has two bound states with a positive-imaginary wave number (negative real energy). The S-matrix poles representing resonances of this real part are symmetric with respect to the imaginary k axis (real E axis), according to Eq. (20). The first two resonances are very close to the real k axis, and therefore very narrow (with widths of about 10^{-13} MeV and 10^{-3} MeV, respectively). The addition of an absorptive (negative) imaginary part to the potential modifies these properties. Normalizable-state k values ($N1$ and $N2$) become complex, with a negative real part (energies have a negative imaginary part). Resonances on the right-hand side of the k plane move away from the real axis and become broader ($R3$' to $R6$'). Some resonances on the left-hand side cross the real axis and change into normalizable states. The first three resonances become square-integrable solutions $N3$ to $N5$ with ReE positive. Consequently, the complex potential has five normalizable solutions. The other resonances remain under the real k axis and become narrower such as $R6$. Resonance energies are not any more symmetric with respect to the imaginary axis. Such a motion of the poles of the S matrix has been qualitatively predicted in Ref. [36].

In Sec. III C, we have examined the influence of the poles of the S matrix on the complex phase shift (see Fig. 2 for a summary). Figure 4 compares the phase shifts of the real part of the potential (thin line) and of the full complex (thick lines) $l=18$ potential. The Levinson theorem (23) is verified in both cases. The phase shift of the real potential starts from 2π at $E=0$ since the potential has two bound states. The complex phase shift starts from 5π at $E=0$ since the complex potential has five normalizable states $N1$ to $N5$. We verified numerically that $\xi^{18}(\infty)=0$ and $A^{18}(\infty)=1$. Let us recall that the Levinson theorem is verified here because the energy dependence of the potential is frozen. Both phases become almost identical beyond 30 MeV in spite of the fact that A^{18} is still far from unity.

The influence of the poles on the phase shift can be seen in Fig. 4. For the real potential, two narrow resonances and a broader resonance clearly appear. For the full complex potential, the influence of the first two resonances disappears. This is due to the fact that the poles $N3$ and $N4$ in Fig. 3 are, respectively, nearly symmetric to $R3$' and $R4$' with respect to the k-plane origin. The phase shift results from a compensation between two opposite behaviors shown in Fig. 2 as discussed in Sec. III C. On the other hand, a broad resonance arises from the pole $R5$', while the associated pole $N5$ changes into a square-integrable state. The resulting effect on the phase shift combines a broad-resonance behavior (Fig. 2, Im$k_0<0$, Re$k_0>0$) and a narrow-normalizable-state behavior (Fig. 2, Im$k_0>0$, Re$k_0<0$). A fast decrease is superimposed on a slower increase in the phase ξ^{18}. The influence of

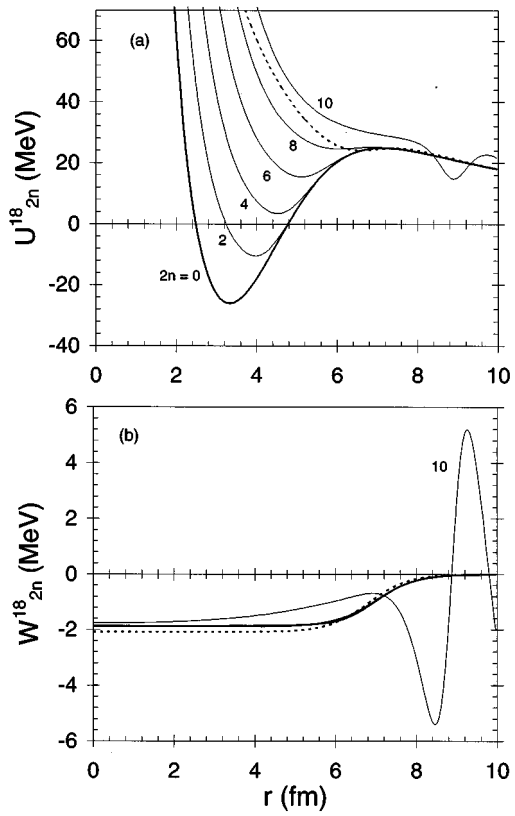

FIG. 5. Real parts U^{18} and imaginary parts W^{18} of the $l=18$ potential V_0^{18} of Ref. [12] (thick line), of the phase-equivalent potentials $V_2^{18},\ldots,V_{10}^{18}$ (thin lines, labeled by $2n$), and of the shallow potential of Ref. [3] (dotted line), at 25 MeV. The imaginary potentials W_2^{18} to W_8^{18} are almost indistinguishable from the initial imaginary part.

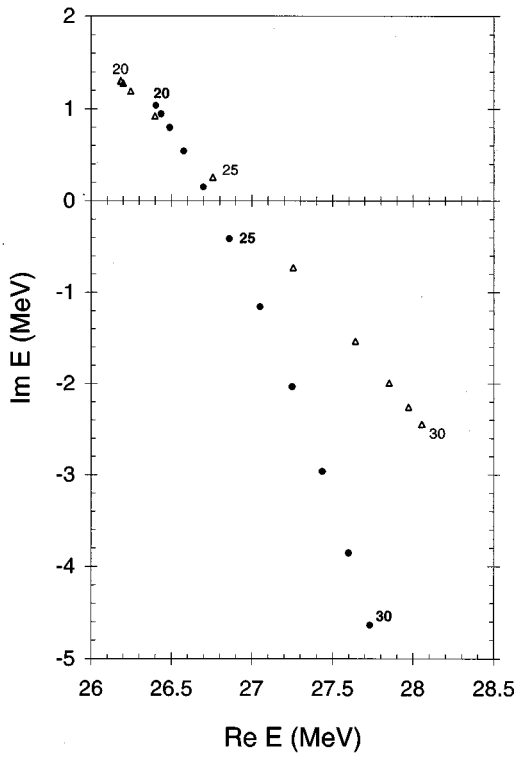

FIG. 6. Energy location of the S-matrix pole which mostly influences the $l=18$ phase shift, for the energy-dependent potentials of Ref. [3] (triangles) and of Ref. [12] (dots), at energies varying between 20 MeV and 30 MeV by 1 MeV steps.

the normalizable state appears to be dominant for A^{18} since the modulus of the S matrix cannot exceed unity.

B. Removal of normalizable states

As an illustration of the method exposed in Sec. II C, we construct a family of potentials which are phase equivalent to the effective potential studied in Sec. IV A (namely the $l=18$, $E=25$ MeV potential of Kondō *et al.*). We remove the states according to increasing real parts of the energy (i.e., we successively remove states $N1, N2, \ldots, N5$ in Fig. 3). The evolution of the potential shape can be followed at each step. The real and imaginary parts of the potentials V_0^{18}, $V_2^{18},\ldots,V_{10}^{18}$ are shown in Fig. 5. For the first four transformed potentials, the comments are identical: the imaginary part of the potential is almost not modified, while the depth of the real part regularly decreases. The last potential V_{10}^{18} is very different. The requirements on this potential are quite restrictive: it has to share the same phase shift as V_0^{18}, but without the normalizable state at $N5$ which has a visible influence on the phase shift in Fig. 4. Consequently, its shape is quite unusual, with oscillations and a much larger extension than for other potentials. Moreover, its imaginary part becomes positive for some ranges of r values. This kind of behavior has already been met and described in Ref. [26]. It occurs according to Eq. (49) of that reference when a removed square-integrable solution is located at some k_0 which satisfies

$$|\mathrm{Im}k_0| \ll |\mathrm{Re}k_0|. \tag{34}$$

However, as shown in Sec. III C, an additional condition is that another pole near $-k_0$ does not cancel its effect. The closeness of $N5$ to the imaginary k axis and the asymmetry between $N5$ and $R5$' are therefore simultaneously responsible for the shape of V_{10}^{18}. In the following, we shall not keep this kind of strange potential.

Figure 5 shows that the potential singularity at the origin increases at each state removal, in accordance with Eq. (31). A positive singular core repels positive-energy wave functions from the origin and simulates in some sense the orthogonality of scattering states with suppressed normalizable states, which themselves simulate the Pauli forbidden states.

Finally, Fig. 5 compares the supersymmetric partners of the deep potential of Kondō *et al.* with the shallow potential of Chatwin *et al.* [3] (dotted line). This last potential is close to potential V_8^{18} obtained by removing four normalizable states from the deep potential. A more detailed comparison between these potentials is done in the next subsection.

In conclusion, a family of regularly shaped potentials which have the same complex phase shifts can be derived with supersymmetric transformations. They approximately share the same absorptive part, but the depths of their real parts and hence the numbers of bound states but also of narrow resonances of these real parts are different. Similar

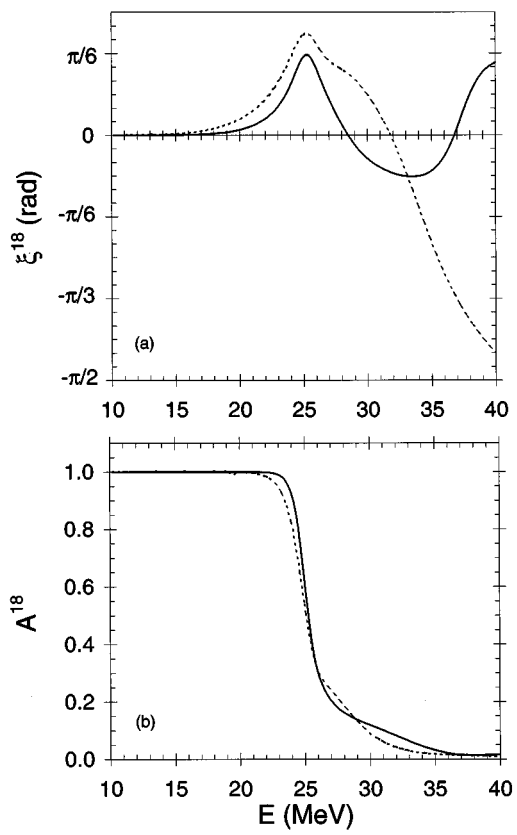

FIG. 7. Phase and modulus of the S matrix for the energy-dependent deep (full lines) and shallow (dotted lines) $l=18$ potentials.

results are obtained for other partial waves, but with a different number of transformations. These families of potentials explain the well-known discrete ambiguity encountered in optical-model fits of heavy-ion elastic scattering cross sections.

C. Energy dependence of the $^{16}O+^{16}O$ potentials

Deep and shallow potentials which correctly reproduce data in the energy range 10 MeV$<E_{\mathrm{c.m.}}<$35 MeV [3,12] have common characteristics: (i) their real part depends neither on energy nor on angular momentum (a slight l dependence exists for the potential of Kondō *et al.*, but a similar potential can be obtained without this dependence [13]), and (ii) the depth of their imaginary part increases with energy according to a parametrization based on a cutoff angular momentum. This type of imaginary part can be criticized with causality arguments based on dispersion relations [38]. This criticism does however not concern the narrow energy domain considered here.

Figure 6 shows the location of the S-matrix pole which mostly influences the $l=18$ phase shift, for both potentials of Chatwin *et al.* (triangles) and of Kondō *et al.* (dots), with $E_{\mathrm{c.m.}}$ varying between 20 MeV and 30 MeV by 1 MeV steps. At the energies where this partial wave dominates, both potentials display a pole at about the same location. Since the depth of the imaginary part of the potential increases with energy, the resonance becomes a normalizable state beyond 25 MeV for the Chatwin potential and beyond 24 MeV for the Kondō potential. For the potential of Kondō *et al.* at 25 MeV, we have already encountered this normalizable state in Sec. IV A (dot $N5$ in Fig. 3), but it is worth insisting on the fact that this state can also be square integrable for the ''shallow'' potential. The main difference between the deep and shallow phenomenological potentials is that this normalizable state is the fifth one for the deep potential, while it is the first one for the shallow potential.

Figure 7 displays the $l=18$ complex phase shifts of the energy-dependent potentials. Here Eq. (1) is solved with a different potential at each energy. Therefore the phase shifts do not verify the Levinson theorem (23). The influence of the S-matrix pole followed in Fig. 6 can clearly be seen: when the energy increases, the number of normalizable states increases and the reflection coefficient decreases towards zero at high energies. Indeed the imaginary part of the potential increases with energy and the reflection coefficient becomes very small over some energy range. The relevant poles of the potential move with energy in such a way that the reflection coefficient remains small at high energies. This kind of behavior also occurs for the other partial waves, but at different energies. Consequently, each partial wave is predominant over a limited energy range, as explained in Ref. [4]. Moreover, the transition between a resonant behavior and a normalizable-state behavior can be seen on the real part ξ^{18} of the complex phase shift, which increases up to 25 MeV and then decreases in agreement with the schematic behavior of Fig. 2.

Figures 6 and 7 clearly reveal similarities between deep and shallow potentials, which explain why they both fit the data so well. The difference between the real phases ξ^{18} at higher energies is not relevant for the cross sections since the reflection coefficient is already very small.

By removing all normalizable states which lead to nonoscillating potentials, the resulting supersymmetric partner of the deep potential of Ref. [12] is very close to the shallow potential of Ref. [3] over the whole energy range considered. The appropriate supersymmetric partners of effective deep potentials $l=12$ to $l=20$, at energies $E_{\mathrm{c.m.}}=20$, 25, and 30 MeV are presented in Figs. 8(a), (b), and (c), respectively. The potentials are close to one another, particularly for the dominant partial waves at each energy, namely $l=12$ and 14 at 20 MeV, $l=16$ and 18 at 25 MeV, and $l=18$ and 20 at 30 MeV.

The characteristics of the transformed potentials are very similar to those discussed in Sec. IV B. The relative difference between the imaginary parts of the initial and final potentials does not exceed 10%. The depth of the real part decreases because of the normalizable-state removals. The singularity at the origin increases in order to maintain the phase shift. Moreover, the effect of supersymmetric transformations on the real part of the potential is almost identical at the three energies. Consequently, the real part of the supersymmetric partner does not depend on energy in this domain, in agreement with a property of the shallow phenomenological potential. This real part depends on angular momentum but can be simulated over a limited energy range by an l-independent potential.

Deep potentials also exist at $E_{\mathrm{c.m.}}=175$ MeV [14] and $E_{\mathrm{c.m.}}=72.5$ MeV [15]. Shallow potentials are not available at these energies. Constructing them with supersymmetry is

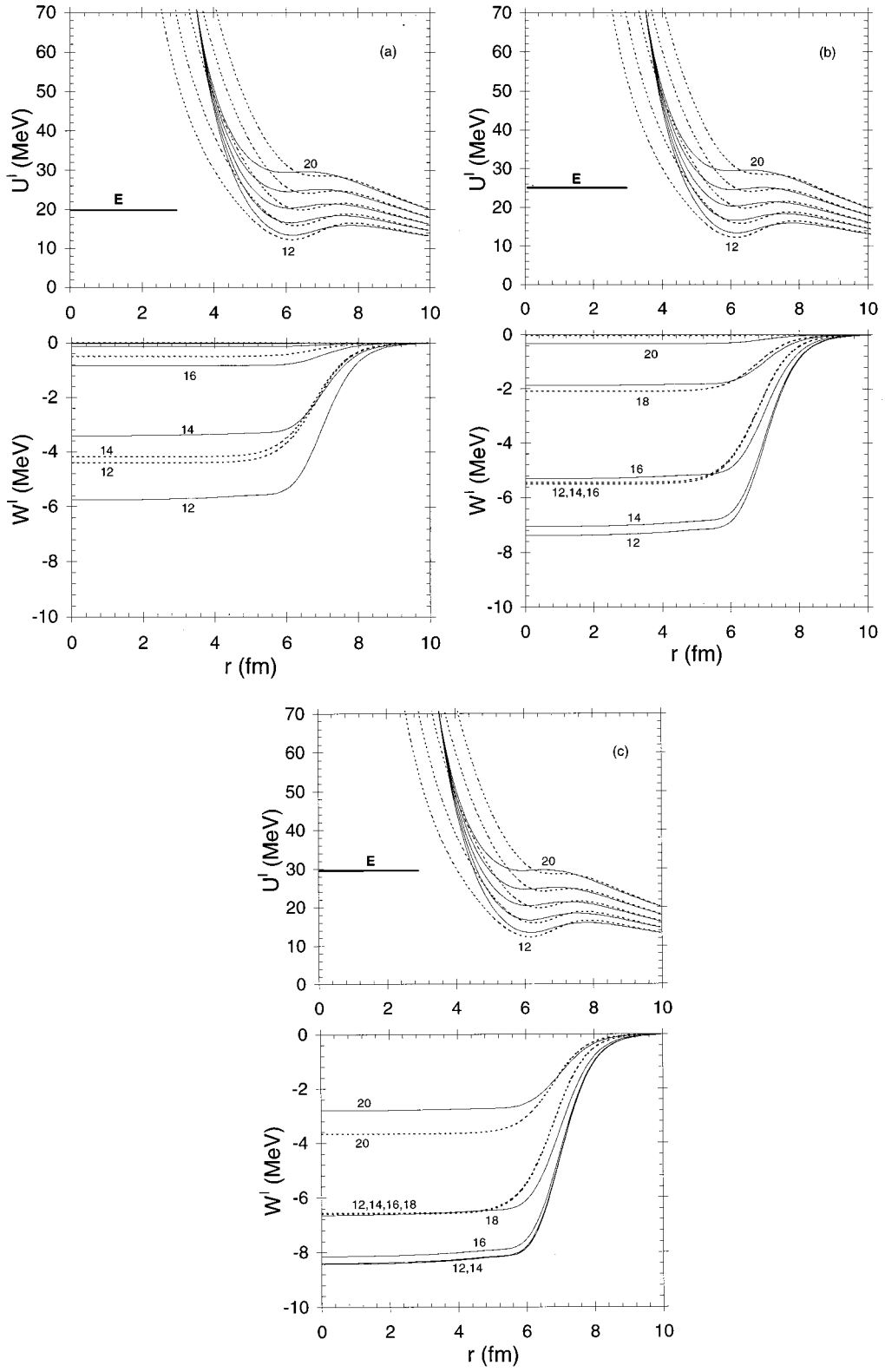

FIG. 8. Supersymmetric partners of effective deep potentials (full lines) and effective shallow potentials (dotted lines) for $l=12$ to 20, at energies $E_{\text{c.m.}}=20$ MeV (a), 25 MeV (b), and 30 MeV (c).

still possible but not very interesting. Indeed, the number of forbidden states predicted by microscopic models is $(24-l)/2$ for l smaller than the critical number 24 for $^{16}\text{O}+^{16}\text{O}$ [5] and zero beyond. Therefore only the potentials of low partial waves for which the reflection coefficient is almost equal to zero would be modified. The dominant partial waves are beyond $l=24$ at 72.5 MeV and at 175 MeV and do not have any forbidden normalizable state or resonance. Consequently, supersymmetry cannot usefully modify the effective potentials for these partial waves.

V. CONCLUSION

The $^{16}O+^{16}O$ system offers an almost perfect example of the practical use of supersymmetry in heavy-ion scattering. The availability of high-quality potentials for both deep and shallow types allows a detailed comparison which leads to a simple explanation of their coexistence. The shallow potentials of Ref. [3] are essentially equivalent to potentials resulting from the removal of most square-integrable states from the deep potentials of Ref. [12]. These normalizable states correspond to bound states but also to narrow resonances of the real part of the potential. The main remaining difference is that the equivalent potentials have a singularity depending on the orbital momentum which does not appear in phenomenological shallow potentials. Because of absorption, this singularity does not significantly affect the phase shifts in the considered energy range.

It is interesting to observe that the real parts of some equivalent complex potentials are very close to the real potentials obtained by removing bound states from the real part only. However in order to reach the final equivalent potential, one should also remove narrow resonances from the real part. This is not possible for purely real potentials since eliminating resonances results in a modification of the phase shifts incompatible with phase equivalence. The introduction of a weak imaginary term provides a way of removing narrow resonances without affecting the rest of the phase shift. Except for its role for narrow resonances, the imaginary part has a rather small influence on the transformation of the real part as already observed for the $\alpha+^{16}O$ system in Ref. [26]. On the contrary, the evolution of the imaginary part, although rather weak, requires a full complex treatment.

We have also taken advantage of the opportunity to clarify different aspects of scattering theory with complex potentials and effects of supersymmetry on such potentials. The behavior of a complex phase shift in the vicinity of a resonance and, more unusually, of a normalizable state has been explained as summarized in Fig. 2. The apparent contradiction between removing a square-integrable solution which corresponds to a pole of the scattering matrix while keeping this S matrix unchanged for phase equivalence has been explained on the transformation of the Jost function.

ACKNOWLEDGMENTS

We acknowledge interesting discussions with G. Lévai during early stages of this work. This text presents research results of the Belgian program on interuniversity attraction poles initiated by the Belgian State Federal Services for Scientific, Technical and Cultural Affairs. J.-M. Sparenberg was also supported by the Fonds National de la Recherche Scientifique of Belgium.

[1] R.H. Siemssen, J.V. Maher, A. Weidinger, and D.A. Bromley, Phys. Rev. Lett. **19**, 369 (1967).
[2] J.V. Maher, M.W. Sachs, R.H. Siemssen, A. Weidinger, and D.A. Bromley, Phys. Rev. **188**, 1665 (1969).
[3] R.A. Chatwin, J.S. Eck, D. Robson, and A. Richter, Phys. Rev. C **1**, 795 (1970).
[4] A. Gobbi, R. Wieland, L. Chua, D. Shapira, and D.A. Bromley, Phys. Rev. C **7**, 30 (1973).
[5] D. Baye and G. Reidemeister, Nucl. Phys. **A258**, 157 (1976).
[6] K. Wildermuth and Y.C. Tang, in *A Unified Theory of the Nucleus*, edited by K. Wildermuth and P. Kramer (Vieweg, Braunschweig, 1977).
[7] Y.C. Tang, in *Topics in Nuclear Physics II*, Lecture Notes in Physics Vol. 145 (Springer, Berlin, 1981), p. 572.
[8] H. Friedrich, Nucl. Phys. **A224**, 537 (1974); A. Tohsaki, F. Tanabe, and R. Tamagaki, Prog. Theor. Phys. **53**, 1022 (1975); D. Baye and P.-H. Heenen, Nucl. Phys. **A276**, 354 (1977); L.F. Canto, *ibid.* **A279**, 97 (1977).
[9] R.G. Newton, *Scattering Theory of Waves and Particles*, 2nd ed. (Springer, New York, 1966).
[10] P. Swan, Proc. R. Soc. London, Ser. A **228**, 10 (1955).
[11] K. Aoki and H. Horiuchi, Prog. Theor. Phys. **69**, 1154 (1983).
[12] Y. Kondō, B.A. Robson, and R. Smith, Phys. Lett. B **227**, 310 (1989).
[13] Y. Kondō, B.A. Robson, and R. Smith, *Proceedings of the Fifth International Conference on Clustering Aspects in Nuclear and Subnuclear Systems*, Kyoto, 1988 [J. Phys. Soc. Jpn Suppl. **58**, 1714 (1989)].
[14] Y. Kondō, F. Michel, and G. Reidemeister, Phys. Lett. B **242**, 340 (1990).
[15] Y. Sugiyama, Y. Tomita, H. Ikezoe, Y. Yamanouchi, K. Ideno, S. Hamada, T. Sugimitsu, M. Hijiya, and Y. Kondō, Phys. Lett. B **312**, 35 (1993).
[16] P. Darriulat, G. Igo, H.G. Pugh, and H.D. Holmgren, Phys. Rev. **137**, B315 (1965).
[17] S. Ali and A.R. Bodmer, Nucl. Phys. **80**, 99 (1966).
[18] V.G. Neudatchin, V.I. Kukulin, V.L. Korotkikh, and V.P. Korennoy, Phys. Lett. **34B**, 581 (1971).
[19] B. Buck, H. Friedrich, and C. Wheatley, Nucl. Phys. **A275**, 246 (1977).
[20] D. Baye, Phys. Rev. Lett. **58**, 2738 (1987).
[21] P. Swan, Nucl. Phys. **46**, 669 (1963).
[22] D. Baye, J. Phys. A **20**, 5529 (1987).
[23] L.U. Ancarani and D. Baye, Phys. Rev. A **46**, 206 (1992).
[24] D. Baye, Phys. Rev. A **48**, 2040 (1993).
[25] D. Baye and J.-M. Sparenberg, Phys. Rev. Lett. **73**, 2789 (1994).
[26] D. Baye, G. Lévai, and J.-M. Sparenberg, Nucl. Phys. **A599**, 435 (1996).
[27] C.V. Sukumar, J. Phys. A **18**, 2917 (1985).
[28] D. Baye and P.-H. Heenen, J. Phys. A **19**, 2041 (1986).
[29] M. Vincke, L. Malegat, and D. Baye, J. Phys. B **26**, 811 (1993).
[30] C. Grama, N. Grama, and I. Zamfirescu, Ann. Phys. (N.Y.) **232**, 243 (1994).
[31] M. Abramowitz and I.A. Stegun, *Handbook of Mathematical Functions* (Dover, New York, 1972).
[32] J.R. Taylor, *Scattering Theory* (Wiley, New York, 1972).
[33] Z.R. Iwinski, L. Rosenberg, and L. Spruch, Phys. Rev. Lett. **54**, 1602 (1985).
[34] B.N. Nagorcka and J.O. Newton, Phys. Lett. **41B**, 34 (1972).

[35] J.S. Duval, Jr., A.C.L. Barnard, and J.B. Swint, Nucl. Phys. **A93**, 164 (1967).
[36] A. Gal, G. Toker, and Y. Alexander, Ann. Phys. (N.Y.) **137**, 341 (1981).
[37] Y.K. Ho, Phys. Rep. **99**, 1 (1983).
[38] S. Ait-Tahar, R.S. Mackintosh, and M.A. Russell, J. Phys. G **21**, 577 (1995).